THE SWEEP-BACK ANGLE AND THE AERODYNAMIC INDUCTION LIKE WING CONTRIBUTIONS TO THE DIHEDRAL EFFECT

P. GILI, Associate Professor
Aeronautical and Space Department, Polytechnic of Turin
Turin - ITALY

Abstract. This study has been designed to fine tune a method for evaluating the contribution of the sweep-back angle and the aerodynamic induction of the wing on the dihedral effect, that is the derivative of the rolling moment coefficient with respect to the side-slip angle. This aerodynamic derivative, determined by at least other four contributions, is important, as widely known, in the study of the side-directional motion of the aircraft, and in particular in the determination of its dynamic characteristics concerning Dutch roll and spiral mode.

We have evaluated these two contributions to C_{l_β} in two different ways. For the sweep-back angle contribution we have used a simple integration method along the span of the single infinitesimal wing element, obviously evaluating the different influences on the two semi-wings when the aircraft is invested by a side-slip angle. For the aerodynamic induction we have used a method which takes into account, also through integration along the span, the different circulation of the two semi-wings each with a different flow situation, again in the presence of a side-slip angle.

This method is Anderson's method modified by us for wings of whatever plant form and with any geometric twist. The effect of the U-vortices, as is well known, consists in inducing a speed at the wing in an orthogonal direction to that of the upstream flow. This induced speed changes both the module and the direction of the upstream speed, thus provoking a reduction of the angle of attack: the induced angle of attack. Anderson's work is based on the solution of Prandtl's integral-differential equation and permits to calculate the circulation on the wing, so that it is possible to define the induced angle of attack along the wing span.

Anderson's method doesn't provide for high swept angle wings and so, as mentioned above for the sweep-back angle contribution, a simple integration along the wing span have been done; it is however our purpose to extend Anderson's method to sweep-back or sweep-forward angle wings.

The results are presented in shape of curves as a function of lift coefficient, being as we know these two contributions to C_{l_β} dependent on the different circulation of the two semi-wings and therefore dependent on the angle of attack.

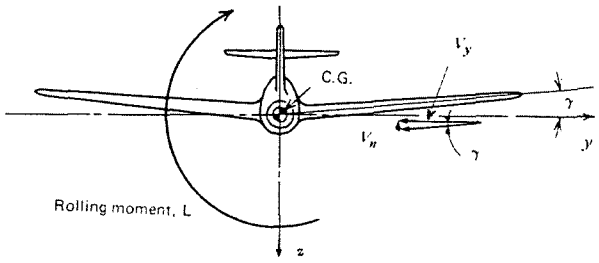

Figure 1: Dihedral wing angle contribution.

Introduction

The derivative $C_{l_\beta} = \partial C_l / \partial \beta$ goes under the name of *Dihedral Effect.* The dihedral angle of the wing, even if it gives its name to this derivative (which actually only explains the fact that the aircraft is subjected to a rolling moment L when it is invested by a sideslip angle β) it is only one of the elements contributing to C_{l_β}.

The dihedral angle γ of the wing, infact, supplies a component of speed, V_n, normal for a quarter line chord and of opposite sign on the two semi-wings. This determines a lift difference between the two semi-wings thus creating a rolling moment L (see Fig.1). For the positive dihedral angle and sideslip angle, this contribution to C_{l_β} is negative.

Another wing element contribution is the interference with the fuselage (Fig.2). According to the wing-body relative position, due to the effect of a sideslip

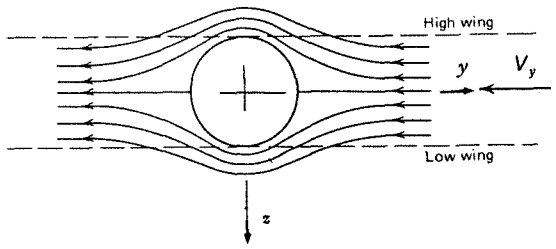

Figure 2: Wing-body relative position contribution.

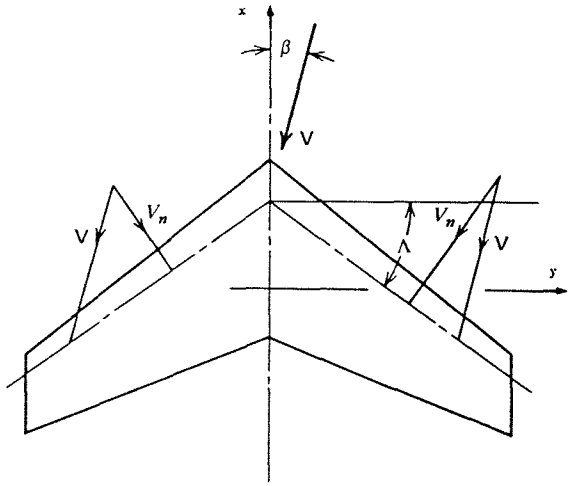

Figure 3: Swept wing angle contribution.

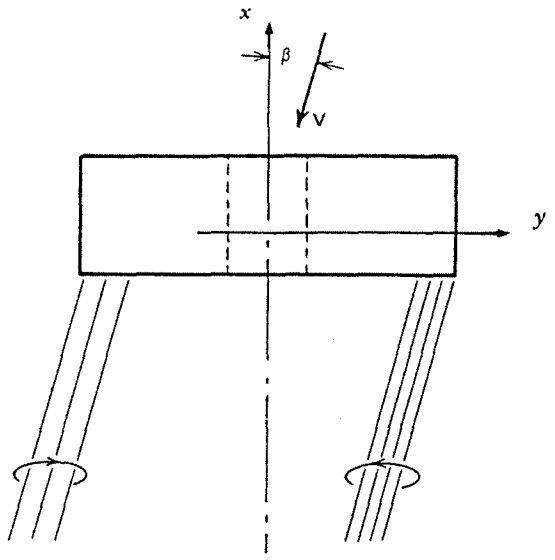

Figure 4: Aerodynamic induction contribution.

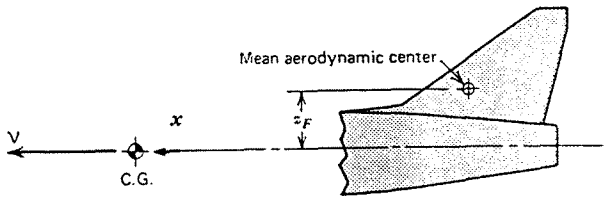

Figure 5: Vertical tail contribution.

angle, a side flow is generated giving it normal components for the wing. These components then bind with the speed V_x according to the body-axis x, generating a lift variation of opposite sign on the two semi-wings. Therefore, another rolling moment is generated that has the opposite sign, according to the wing-body relative position and obviously according to the direction of the sideslip angle, that means according to its sign.

The swept wings also contribute to C_{l_β} (Fig.3). A sweep-back angle Λ supplies a speed component V_n, that is useful aerodynamicly because is normal for the quarter line chord, and is different on the two semi-wings. This situation generates, like the cases above-mentioned, a lift difference for the two semi-wings and therefore a rolling moment. C_{l_β} in this case is negative with sweep-back angles.

Even if a straight wing is invested by a sideslip angle it can produce a rolling moment (Fig.4). Infact, two wing sections equidistant from the symmetrical plane, have different distances from the global U-vortex wing system and particularly from the vortices of the tip wing. This is the reason why the induced speed and therefore the induced angle of attack is averagly different on the two semi-wings. This event always causes a lift difference of the two semi-wings and, therefore generating a rolling moment. In this case the contribution to C_{l_β} is positive together with a positive sideslip angle.

Another wing element contribution to C_{l_β} is the shape of the tip of the wing. Anyway, this contribution can be omitted even when the wing has winglets.

Besides the wing, the vertical tail (Fig.5) contributes considerably to the C_{l_β}. When the aircraft collides with a sideslip angle, the vertical tail generates a side force. If the mean aerodynamic center, that is the point where the side force is applied, is fairly distant from the rolling axis, the side force itself generates a rolling moment. Also in this case the contribution to C_{l_β} is negative with positive sideslip angles.

If external bodies, like nacelles or floats, which differ from the fuselage, are fastened to the aircraft, when a sideslip angle is present they are subjected to a side force. If it has a lever arm with a certain entity from the x-axis, even in this case a rolling moment will be generated. However, these contributions are usually omitted, except when the aircraft has a particular shape.

Amoung these contributions, three of them have the same order of size: swept wing angle, dihedral wing angle and vertical tail which can reach at the most same tenth (obviously with angles of a certain entity and conventional vertical tail). The wing aerodynamic induction contribution is of a smaller size (and in any case it depends on the C_L of flight), while the wing-body relative position contribution is of two order smaller and the contribution of the shape of the tip of the wing is even of three order smaller.

Various authors [2, 3, 5] have worked out simple formulas in order to estimate at least three of the contributions that really count, that are: the contribution of the dihedral wing angle, the wing-body relative position and the vertical tail. Even if it does exist, it is easy to estimate, in the same way of that for the vertical tail, also the contribution of the external bodies fastened to the aircraft. The Etkin [2] also reports, unless a constant, a relation to estimate the swept wing angle contribution (which also depends on the C_L of flight).

During these studies, a complete formula was reached, even if very simple and approximate, for the swept angle contribution to C_{l_β} and we estimated, through Anderson's method, the contribution to the C_{l_β} of different aerodynamic induction of the two semi-wings which are invested with a sideslip angle.

Anderson's method, as explained in the following paragraph, has been extended in order to be applied to wings having any plant form and any twist, but at the moment it can only be applied straight wings or with low swept angles.

A swept-tapered wing was used for our calculations and as a numerical example, therefore the swept angle contribution and the tapered wing contribution were considered distinctively and then added, even if, for the tapered wing contribution, the wing could have been straight, but with any plant form and any twist.

Anderson's Method and its Improvements

Anderson's work is based on the solution of Prandtl integral-differential equation, wich originates from the following relation between the angle of attack, the induced angle of attack and the section lift coefficient:

$$\alpha_i = \alpha_a - \frac{c_l}{m_o} \qquad (1)$$

Recalling the circulation expression on the wing, wich is:

$$\Gamma(y) = 2\,b\,V\,g(\theta) \qquad (2)$$

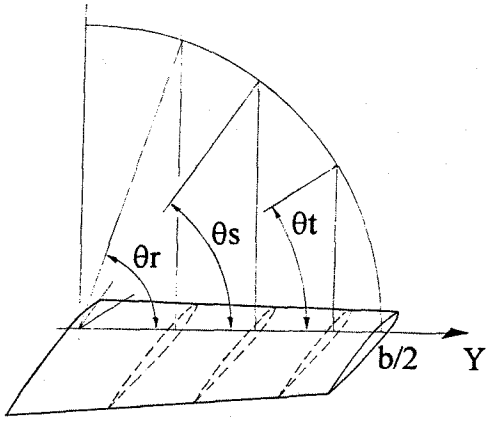

Figure 6: Reference system used by Anderson.

and introducing Fourier series instead of $g(\theta)$, we obtain the following expression:

$$\Gamma(y) = 2\,b\,V \sum_{n=1,3,5\ldots}^{\infty} A_n \sin(n\theta) \qquad (3)$$

Everything is known in it, but coefficients A_n are the values we want to find. For this purpose we express α_i and c_l in function of $\Gamma(y)$ and replace α_a with a simple geometric relation, obtained supposing the law of the aerodynamic twist to be linear: $\alpha_a = \alpha_{as} + \varepsilon^{rad} \mid \cos\theta \mid$. It results in the following expression:

$$\sum_{n=1,3,5\ldots}^{\infty} A_n \sin(n\theta) \left[\frac{n}{\sin\theta} + \frac{4b}{c\,m_o}\right] = \alpha_{as} + \varepsilon^{rad} \mid \cos\theta \mid \qquad (4)$$

The term on the right represents the linear law of twist mentioned before. All terms, except the values A_n are known. The method correctness depends upon the number of terms of the series we consider. Anderson has taken the first four terms. Consequently, the equation has four unknown quantities (A_1, A_3, A_5 and A_7) whose values can be found if we write it in correspondence of four different wing sections (or of three wing sections with reference to the Fig.6).

The resulting system is defined and linear and, if we considere only three sections (r, s and t), it could be schematized as follows:

$$\begin{aligned} A_1 c_{11} + A_3 c_{12} + A_5 c_{13} &= \alpha_{as} + \varepsilon^{rad} \mid \cos\theta_r \mid \\ A_1 c_{21} + A_3 c_{22} + A_5 c_{23} &= \alpha_{as} + \varepsilon^{rad} \mid \cos\theta_s \mid \\ A_1 c_{31} + A_3 c_{32} + A_5 c_{33} &= \alpha_{as} + \varepsilon^{rad} \mid \cos\theta_t \mid \end{aligned} \qquad (5)$$

where c_{ij} represents the quantity we can find on the left hand side of the expression (4), obviously except A_n. Anyway, looking at the system itself, we can observe that values of unknown quantity like A_n are linked to the incidence of the wing (α_{as}) and to its

angle of twist (ε). For each value they assume, we find a different solution of the system wich, of course, brings to a different expression of $\Gamma(y)$. To avoid redoing the whole process for each configuration (once that the wing geometry has been established), Anderson has introduced the following substitution:

$$A_n = B_n \alpha_{as} + C_n \varepsilon^{rad} \qquad (6)$$

Once that the six values (B_n and C_n) have been found, they can be inserted into the expression of $\Gamma(y)$ which, in the meanwhile, has been written in function of them. After that, starting from $\Gamma(y)$, we can obtain all the other quantities concerning the wing (c_{lb} and c_{la} distributions, $x_{a.c.}$, C_{Di} and so on; refer to Anderson's report).

Values of B_n and C_n have been calculated by Anderson for a number of a straight-tapered wings and substituted in the dimensionless quantities L_a and L_b which represent c_{la} and c_{lb} respectively. Besides all the other quantities have been taken into account, but we don't mention them. Results form groups in tables or graphics that are easy to read and by which you can obtain the information you need quite rapidly. The wings studied have rounded tips, their aspect ratios are included between 2 and 20 and their taper ratios are included between 0 and 1.

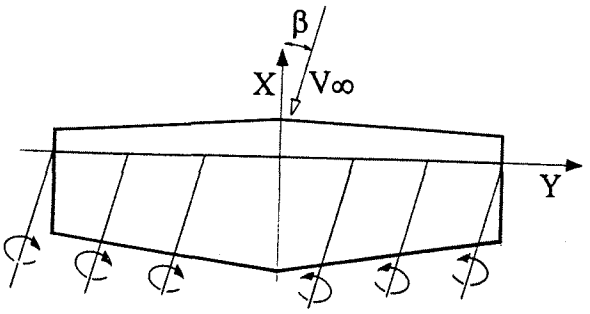

Figure 7: Position of vortex axis in presence of β.

the one obtained whith the wing secion distribution chosen by us. After this, we took a wing of any shape and, in correspondence of chosen sections, we calculated the b/c ratios putting them in the correspondent equation of the system (4). A comparison whith an empiric relation of L_a given by Anderson, has proved the correctiveness of the procedure. Secondly, new laws of twist have been introduced: exponential law or, dividing the semi-wing in two parts (chosen at pleasure) each of them characterized by different a linear law or by different exponential laws. To obtain this, we had to modificate the equations used; now let's see how the law of twist actually changes the expressions in math. The math expressions are contained in Table 1.

	law	resulting equation
linear	$\alpha_a = \alpha_{as} + \varepsilon^{rad}\lvert\cos\theta\rvert$	$C_1 \cdot c_{11} + C_3 \cdot c_{12} + C_5 \cdot c_{13} = \lvert\cos\theta\rvert$
exponential	$\alpha_a = \alpha_{as} + \varepsilon^{rad}\lvert\cos\theta\rvert^n$	$C_1 \cdot c_{11} + C_3 \cdot c_{12} + C_5 \cdot c_{13} = \lvert\cos\theta\rvert^n$
bilinear	1) $\alpha_a = \alpha_{as} + \varepsilon^{rad}\dfrac{\varepsilon_1^{rad}}{\varepsilon^{rad}}\dfrac{\lvert\cos\theta\rvert}{\lvert\cos\theta 1\rvert}$	$C_1 \cdot c_{11} + C_3 \cdot c_{12} + C_5 \cdot c_{13} = \dfrac{\varepsilon_1^{rad}}{\varepsilon^{rad}}\dfrac{\lvert\cos\theta\rvert}{\lvert\cos\theta 1\rvert}$
	2) $\alpha_a = \alpha_{as} + \varepsilon^{rad}\dfrac{\varepsilon_1^{rad} + \varepsilon_2^{rad}\dfrac{X - X1}{1 - X1}}{\varepsilon^{rad}}$	$C_1 \cdot c_{11} + C_3 \cdot c_{12} + C_5 \cdot c_{13} = \dfrac{\varepsilon_1^{rad} + \varepsilon_2^{rad}\dfrac{X - X1}{1 - X1}}{\varepsilon^{rad}}$

Tab. 1: Law of wing twist for different configurations and consequent modifications.

The possibility given to us through the computer, to resolve many complicated systems in a short time, has allowed us to make some improvments on the method. Essentially they have been made in two directions: extension of it to wings of every shape (not only straight-tapered), and the possibility to use a twist charaterized by different laws.

First of all, anyway, it is necessary to look for the correct position of the sections of the wing taken into consideration. This research was based on the comparison between the L_b state given by Anderson and

Aerodynamic Induction Contribution

Our approach in order to take into account the contribution of aerodynamic induction to C_{l_β}, is to consider the wing characterized by the usual group of vortex, shaped like a 'U', with their lateral axis oriented parallely to the wind, as the image shows, therefore forming an angle β whith the wing x-axis (Fig.7).

This changement has an important consequence: the corresponding distribution of section angle of at-

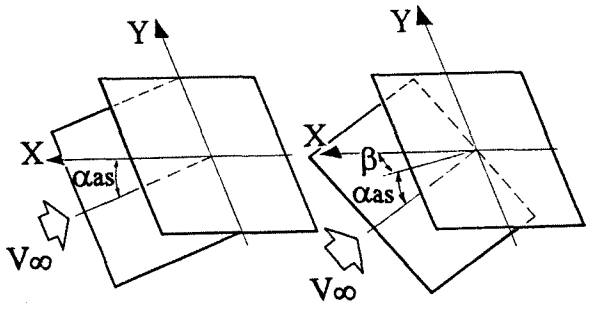

Figure 8: Scheme which represents how α_{as} remains unchanged with β.

tack changes, being translated on the left of a quantity dependent from beta and from the chord of the section we consider, as we will see later. Once that we have found the new induced angle of attack in correspondence of a section, we subtract it to the apparent angle of attack its value obtaining the true angle of attack. Then, multiping it by the wing section lift-curve slope,we find the section lift-curve coefficient:

$$\alpha_e = \alpha_a - \alpha_i = \frac{c_l}{m_o}$$

and so:

$$c_l = m_o\,(\alpha_a - \alpha_i) \qquad (7)$$

The fact is that in presence of angle β, the wing's apparent angle of attack is invariated which can be easily understood looking at the scheme below. The horizontal plane is the plane on which all wing chords lie (there is neither aerodynamic twist nor dihedral). The inclined plane represents the direction of thewind in two cases: when β equals zero and when β is different from zero. It is easy to see that α_{as} is always the same (Fig.8).

Once that we know the section lift coefficient, through an integration we can determine the rolling moment which ought to be the new distribution. Now let see how the calculations ares pratically done. First of all we take into consideration the expression of α_i as it appears in Anderson's method:

$$\alpha_i = \sum_{n=1,3,5\ldots}^{\infty} n\,A_n \frac{\sin(n\theta)}{\sin\theta} \qquad (8)$$

With the computer program realized to use and improuve Anderson's method, we can determine coefficients A_n, consequently we are able to know, for different angle of attack, the distribution of α_i along the span. Than we have to consider the translation caused by β explained before. If we had a wing characterized by a taper ratio equal to one, the situation would be that illustrated in Fig.9.

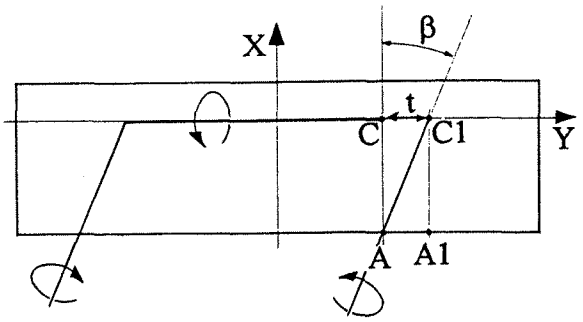

Figure 9: Translation of α_i on the trailing edge in the case of $r = 1$.

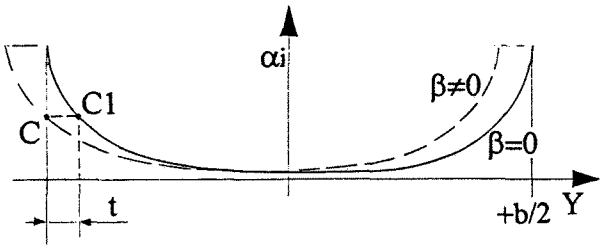

Figure 10: α_i along the span with and without β.

We consider that in presence of side sleep angle the section wing induced angle of attack in A is the same as that we have in A_1 in case of symmetrical flow; so the new situation can be showed with a graphic in which each value of α_i is translated on the left of a quantity equal to t, whose value is given by this relation: $t = 3/4\,c\,\tan\beta$ (see Fig.10), and it is the same for each abscissa y.

If our wing has a taper ratio smaller than one, the situation changes quite a lot. In fact in this case the chord changes linearly along the semispan, consequently the segment t will the same (see Fig.11).

The result in α_i/y graphic, is similar to the previous one, but not equal. Besides it is clear too that on the right tip there is a little portion of surface (delimited by k) which lies on the right of the axis of the

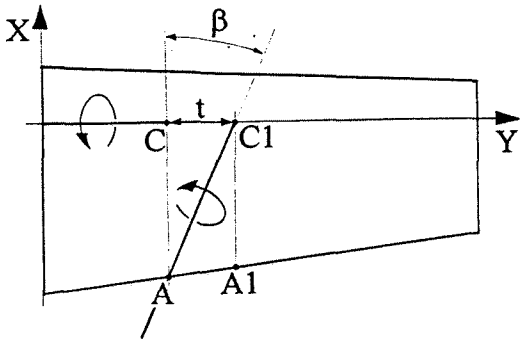

Figure 11: Translation of α_i on the trailing edge in case of $r < 1$.

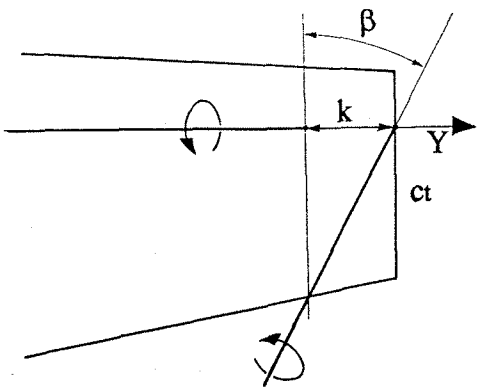

Figure 12: Portion of trailing edge of the right tip.

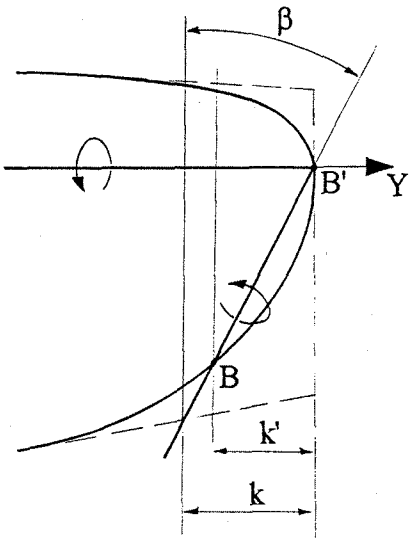

Figure 13: Situation on the right tip in the case it is tapered.

last vortex, so the value of α_i in it remains undetermined. Its amplitude is linked obviously to β, and to the taper ratio too (see Fig.12).

In fact if we observe from nearby the wing tip, it is easy to understand that the dimension of segment k is approximately equal to: $k = 3/4\, c_t \tan\beta$. In spite of its small dimension, it is giving much importance because of the long distance which separates it from x-axis around which we calculate the resulting moment.

Some attempts have proved that, calculating the moment considering a law of α_i distribution instead of another, brings to a completely different result. The problem has been resolved as follows: first of all we have to consider that the tip is rounded and so the segment k is ulteriorly reduced as the drawing confirmes (see Fig.13).

In presence of taper the segment k becomes k' with the conseguent reduction of the area which is

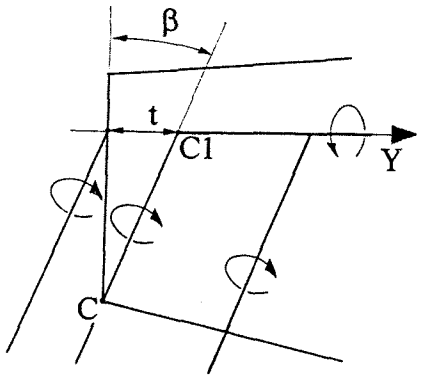

Figure 14: Situation on the left tip.

interested by the undetermined law. Than we must think that the point B lies on the same vortex axis on which B' lies too; consequentely, in both points the induced angle must be the same. Necessarily in the space between B and B' the angle α_i can't change in a radical way, so we can say it is an acceptable approximation if we consider it constant.

The fact of having introduced rounded tips has a consequence also on the left tip. Going back to the previous situation, considering its extreme point C, the corresponding value of α_i is the one which, in case of symmetrical flow, belongs to the point $C1$. Consequently it is smaller, and on the left wing the maximum value of α_i is lost while it continues to be present on the right one (see Fig.14).

Introducing the rounded tip, the situation on it changes quite a lot. In fact the segment t whose α_i graph we have to translate, becomes smaller and smaller till the left end where its value is equal to zero. So the corresponding induced angle in that point is the same we have in the symmetrical situation. The graphic can show the difference (see Fig.15).

Now that we have the value of α_i for each section, using the passages mentioned before, we can obtain the corresponding values of C_l.

From this, with reference to Fig.15, it is possible to calculate the value of the rolling moment coefficient. The moment is given by the following expression:

$$L_{ind} = \frac{1}{2}\rho V^2 \int_{-b/2}^{b/2} c_l\, c\, y\, d(y) \qquad (9)$$

and consequently the coefficient becomes:

$$C_{l_{ind}} = \int_{-b/2}^{b/2} \frac{y}{b/2}\,\frac{1}{2}\,c_l\,\frac{c}{c_m}\,d\left(\frac{y}{b/2}\right) \qquad (10)$$

and with the position: $y/(b/2) = t$ the integral becomes:

$$C_{l_{ind}} = \frac{1}{2}\int_{-1}^{1} t\, c_l\,\frac{c}{c_m}\,dt \qquad (11)$$

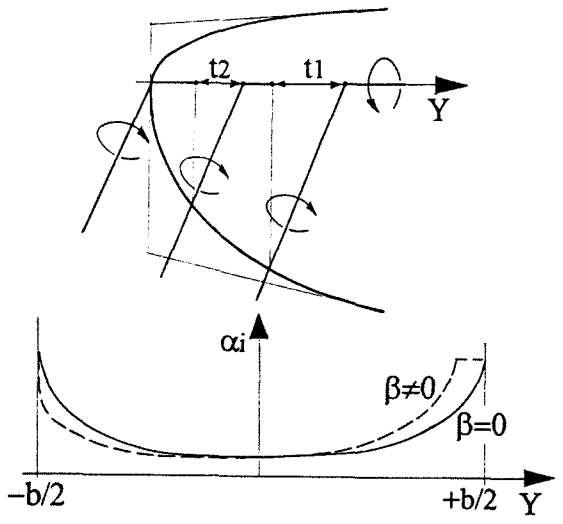

Figure 15: Left tapered tip: reduction of t and consequent α_i distribution.

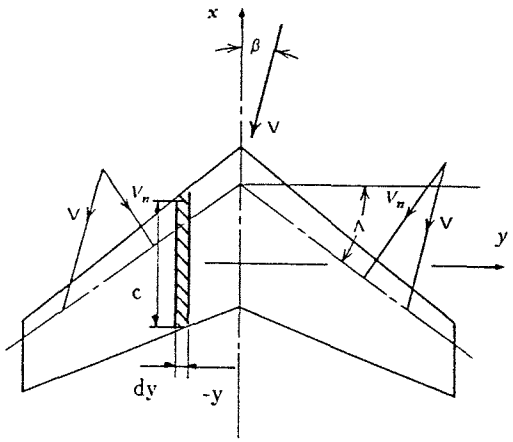

Figure 16: Calculation of the swept wing contribution.

The ratio c/c_m can be expressed in function of the taper ratio and the aspect ratio in this way:

$$\frac{c}{c_m} = \frac{2}{(1+r)}\left[1 + (r-1)t\right] \qquad (12)$$

Taking origin from this expression the computer calculates the value of the coefficient of rolling moment.

Sweep-Back Angle Contribution

As aforementioned in the Introduction, a wing swept angle determines, when the wing is invested by a sideslip angle β, a rolling moment L.

With reference to Fig.16 and considering the two semi-wings invested by the wind effective component V_n, that is, by the component of the wind normal to the quarter line chord, we can write the relation of rolling moment L_Λ caused by the sweep-back angle Λ, when the wing is invested by β. The contributions of the two semi-wings must be considered separately, because each (of the two semi-wings) presents a different effective component of the wind V_n:

$$L_\Lambda = -\int_0^{b/2} \frac{1}{2}\rho V^2 \cos^2(\Lambda-\beta)\, C_L\, c\, y\, d(y) + \\ + \int_0^{b/2} \frac{1}{2}\rho V^2 \cos^2(\Lambda+\beta)\, C_L\, c\, y\, d(y) \qquad (13)$$

The symbols which appear in these integrals are known; see the *List of Symbols* at the end of this report for reference. The signs + and − for the contributions of the two semi-wings are obviously due to the fact that such contributions are opposite and we have followed the usual conventions concerning the rolling moment. For the calculation of this contribution to dihedral effect we have followed the classic method of integration along the wing span of the contributions of single wing elements.

By extracting from the integral what can be considered as constant (for C_L this is only possible by considering the wing with constant aerofoil section and without twist), and by indicating by:

$$I_1 = \int_0^{b/2} c\, y\, d(y)$$

we obtain the following expression of the rolling moment:

$$L_\Lambda = -\frac{1}{2}\rho V^2 C_L I_1 \left[\cos^2(\Lambda-\beta) - \cos^2(\Lambda+\beta)\right] \qquad (14)$$

and, by developing the trigonometric expression in square brackets, we obtain the coefficient:

$$C_{l_\Lambda} = -\frac{2C_L I_1 (4\cos\Lambda \sin\Lambda)}{Sb}\beta \qquad (15)$$

In order to get to this expression by developing the trigonometric expression, one needs to presume that the β angle is small,and therefore: $\cos\beta = 1$ and: $\sin\beta = \beta$; finally, with a furter trigonometric step:

$$C_{l_\Lambda} = -\frac{4C_L I_1 \sin(2\Lambda)}{Sb}\beta \qquad (16)$$

From which the contribution to dihedral effect is obtained:

$$C_{l_{\beta\Lambda}} = -\frac{4C_L I_1 \sin(2\Lambda)}{Sb} \qquad (17)$$

with negative sign, as already mentioned, positive β and sweep-back angle.

C_{l_β} is therefore, due to the wing swept angle, a linear function of C_L with this approximate calculation which sums up all contributions of the single wing elements. In facts, the same result has been achieved also in [2].

For the numerical examples quoted in this work, we have considered a swept-tapered wing, so that integral I_1 takes on a particularly simple form:

$$I_1 = \frac{b^2}{12}\left(c_t + \frac{c_r}{2}\right)$$

Therefore, the (17) takes on the following shape:

$$C_{l_{\beta\Lambda}} = -\frac{4C_L \sin(2\Lambda)(r+1/2)}{6(r+1)} \qquad (18)$$

See the *List of Symbols* for the meaning of the various terms. It is interesting to note that, with the analytic development described above, this contribution to C_{l_β} does not dependon the wing aspect ratio A, but on the wing taper ratio r only.

Results and Numerical Examples

Starting from the relations seen before, we have done a numerical example based on a wing having an aspect ratio equal to 7 and another equal to 5 and a taper ratio equal to 0.5. For our wing $\varepsilon^{rad} = 0$, so $\alpha_a \equiv \alpha_{as}$. The wing firstly has been considered without swept and in this configuration we have calculated the effect of induction in case of sidesleep angle. The angle in question assumes four values: 4°, 8°, 12° and 16°, and for each of them the corresponding value of $C_l = f(\beta)$ has been calculated. The same process has been done with regard to four different absolute wing angles of attack. In Figs. 17 and 18 we can show the $C_l(\beta)$ trends for the four values of α above mentioned.

As we can see, the function $C_l = C_l(\beta)$ is not linear. In consideration of our necessity to obtain a constant value of $C_{l_\beta} = \partial C_l/\partial\beta$, just to make some approximative considerations around the contribute given by the two effects taken in exam, we have to consider the straight line which interpolates the function and to use it in the place of the function itself (its values will use after).

Values of $C_l(\beta)$ are all positive, and change also in dependence of the wing angle of attack. These concepts are summed up in the three-dimension graph which follows (see Fig.19).

It is clear that the coefficient of rolling moment can increase both in dependence of α_{as} that of β.

Later we have taken into exam effects of swept indipendently from induction and, whith a calculus

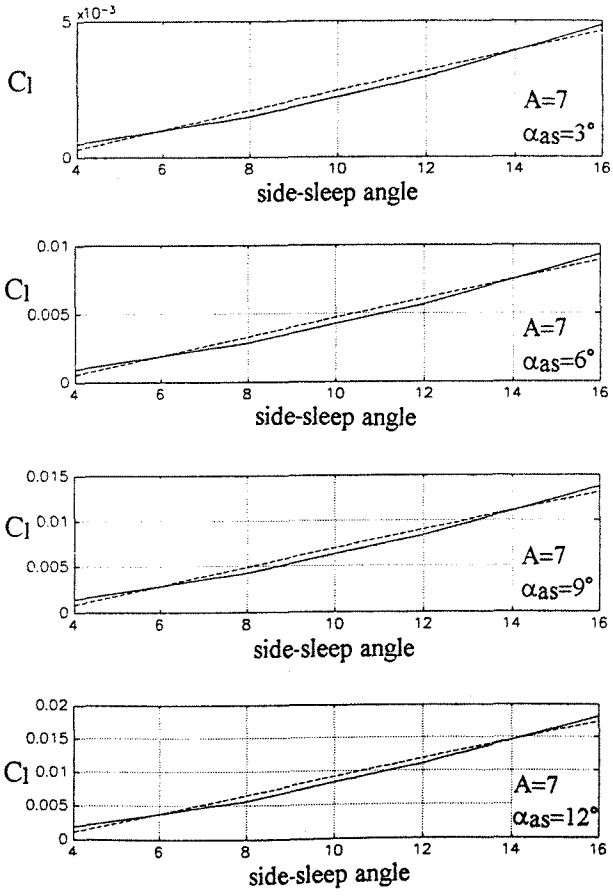

Figure 17: C_l as a function of β for $A = 7$ and for different α.

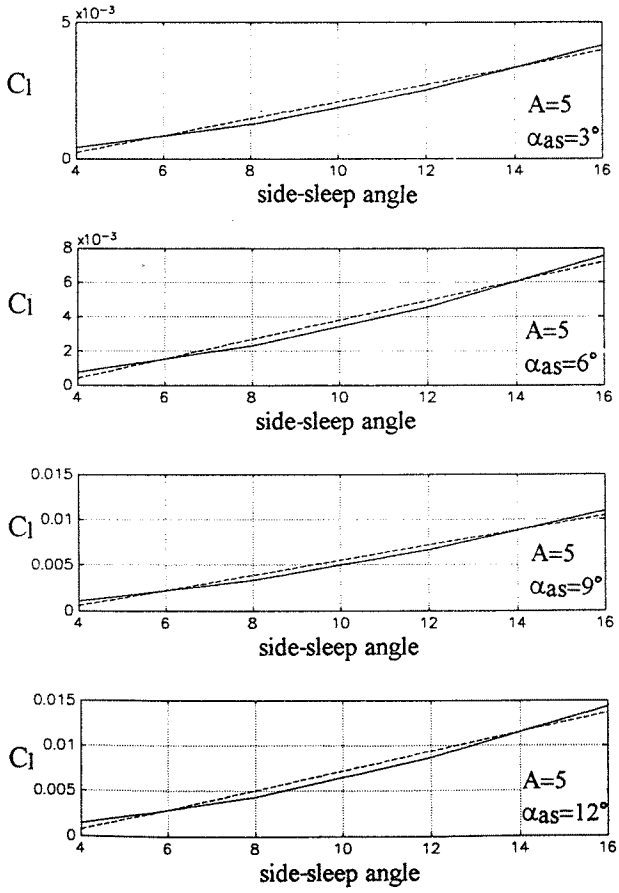

Figure 18: C_l as a function of β for $A = 5$ and for different α.

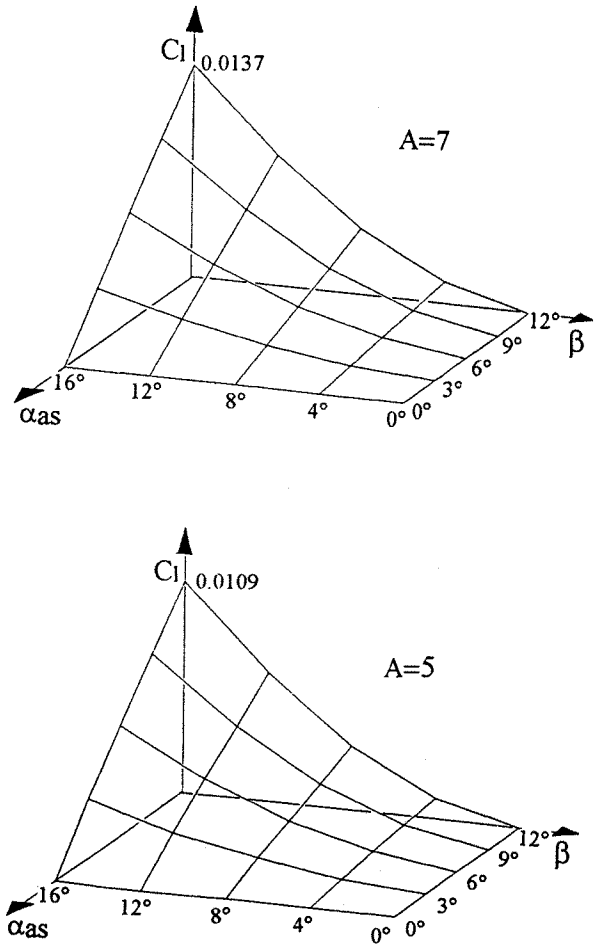

Figure 19: Relation between C_l and the two parameters β and α_{as}.

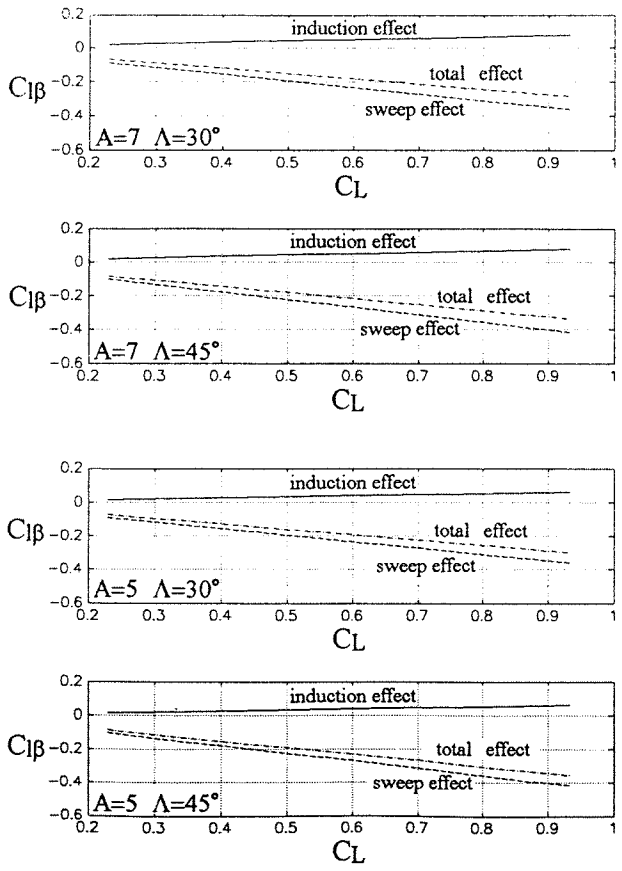

Figure 20: Final results: relation between C_{l_β} and C_L for various configurations.

based on the relation seen before (see paragraph: *Sweep-Back Angle Contribution*), we have obtained the value of C_{l_β}/C_L for two configurations: swept = 30°, swept = 45°. This ratio results indipendent from any other parameter but the taper ratio and the swept. So, in this case, it is constant for any value of C_L and α_{as}. Naturally its sign is negative, opposite to the sign of the same ratio regarding the effect of induction.

Coming back and looking to the relation between C_{l_β} and C_L given by induction, and particulary looking at the function $C_{l_\beta}/C_L = f(C_L)$, we can easily observe that it is almost constant (see Fig.20).

In the some Fig.20 is also reported the sweep-back angle contribution and the sum of the two effects: aerodynamic induction and sweep-back angle.

So, as we have done before, we take in consideration a middle value of the ratio C_{l_β}/C_L to compare it with the correspondent ratio ought to the swept. The contribution linked to the sweep-back angle will be constant for different values of the aspect ratios (like must be as said before). At the same time considering the effect of the aerodynamic induction, the contribution is the same for different angles of swept: in fact thinking about our hypotesis, which consist in studing the two effects separately and summing up their contributes, this second effect has been studied on a wing in which swept is equal to zero. We obtain that reported in Table 2.

	Λ=30°		Λ=45°	
	A=7	A=5	A=7	A=5
$\frac{C_{l\beta_{ind}}}{C_L}$	0.0857	0.0772	0.0857	0.0772
$\frac{C_{l\beta_\Lambda}}{C_L}$	-.3849	-.3849	-.4444	-.4444
$\frac{C_{l\beta_{ind+\Lambda}}}{C_L}$	-.2992	-.3077	-.3587	-.3672

Tab. 2: Final results comprehensive of aerodynamic induction and sweep-back angle.

Conclusions

The above reportes results are quite satisfactory if compared to [7] where diagrams are provided in order to determine the contribution to C_{l_β} for swept-tapered wings (like those considered here) for different aspect ratios and sweep-back angles. It is obvious that the influence of the aspect ratio, in our case, derives from the very aerodynamic induction, given the fact that, as already mentioned, with the simplified development carried out by us, the effect of swept angles is not affected by aspect ratios.

Of course, the integration along the span has involved a large approximation, in that by taking into account the wing elements the reciprocal influence of each other and, most of all, the effect of the wing tip. We have taken this effect into account in the different aerodynamic induction of the two semi-wings, and it is interesting to note that the effect of aerodynamic induction is far from negligible in the evaluation of the various contributions of the wing to C_{l_β}.

Another large approximation has been introduced by considering the β angle as always small, so that, if confounding the angle with the sine involves the great comfort of having a C_{l_β} independent from β, it is also true that $\cos\beta$ may become quite different from 1.

We intend to carry out a test in the wind tunnel of our Department at the Polytechnic of Turin on

a isolated swept-tapered wing. In this way we will obtain an immediate confirmation of the accuracy of our results, as well as an indication of the possible variation range of the involved parameters, so as to provide constant precision of the results.

The next development of this work will consist in the attempt to extend Anderson's method to swept wing with dihedral angle. Twist angles can already be taken into account thanks to the above mentioned extension of Anderson's method. By so doing, we will be able to determine all contributions of the wing to the dihedral effect and to consider wings of any shape and geometry.

List of Symbols

A	Aspect ratio
b	Wing span
c	Local chord
c_l	Section lift coefficient
c_{la}	Section additional lift coefficient
c_{lb}	Section basic lift coefficient
c_m	Mean geometric chord
c_r	Wing root chord
c_t	Wing tip chord
C_{Di}	Wing induced drag coefficient
C_l	Rolling moment coefficient
C_{l_β}	Dihedral effect $= \partial C_l / \partial \beta$
C_L	Wing lift coefficient
L	Rolling moment
m_o	Wing section lift curve slope
r	Wing taper ratio $= c_t/c_r$
S	Wing area
V	Wind speed $= V_\infty$
V_n	Normal wind speed component
V_x	Wind speed component along x-axis
V_y	Wind speed component along y-axis
V_z	Wind speed component along z-axis
x, y, z	Body axes
$x_{a.c.}$	Co-ordinate of wing aerodynamic center
X	Generic co-ordinate of a wing section $= \cos\theta$
X_1	Co-ordinate of a wing section of twist law change $= \cos\theta_1$
α_a	Section apparent angle of attack
α_{as}	Absolute wing angle of attack measured from the zero lift direction of the root section
α_e	Section effective angle of attack
α_i	Section induced angle of attack
β	Sideslip angle
γ	Wing dihedral angle
ε^{rad}	Twist in radiants from root to tip
ε_1	Twist from root to the section of twist law change
ε_2	Twist from the section of twist law change to tip
θ	Anomaly
Λ	Swept wing angle
ρ	Air density

References

[1] R.F. Anderson, *Determination of the Characteristics of Tapered Wings*, NACA TR 572, 1936.

[2] B. Etkin, *Dynamics of Flight - Stability and Control*, John Wiley & Sons, New York, Second edition, 1982.

[3] A. Lausetti, F. Filippi, *Elementi di Meccanica del Volo*, Levrotto & Bella, Torino, 1956.

[4] R. Marini di Villafranca, *Aerodinamica dell'Ala in Basso Subsonico*, Giorgio Editore, Torino, 1971.

[5] C.D. Perkins and R.E. Hage, *Airplane Performance Stability and Control*, John Wiley & Sons, New York, 1949.

[6] F. Quori, *Aerodinamica*, Levrotto & Bella, Torino, Sett. 1993.

[7] Royal Aeronautical Society, *Data Sheet Aircraft*, 06. 01. 04.